Inverterless High Power Interior Permanent Magnet Automotive Alternator

W.L. Soong and N. Ertugrul
University of Adelaide
Adelaide, Australia

Abstract : **This paper describes a high power brushless interior permanent magnet (PM) automotive alternator which does not use an inverter. The "inverterless" alternator is designed with a high back-emf voltage and high reactance, and thus operates as a constant current source over much of its wide constant power operating speed range. In this configuration, a switched-mode rectifier is used to regulate the DC output voltage and current, which avoids the complexity and high cost of an inverter. The analysis of the modelling and performance of interior PM machines for this inverterless topology is described and experimental results are presented for a 6kW concept demonstrator machine showing an outstanding constant power speed range.**

I. INTRODUCTION

Conventional car alternators are based on a three-phase (3-ph) Lundell type wound-field synchronous alternator with a 3-ph rectifier (see Fig 1a). The output voltage is regulated by adjusting the field current. These alternators are simple and low-cost (production cost about US$75) [1]. They are, however, limited in output power to about 1-2kW (see Fig. 2a) due to scalability and efficiency issues. Other limitations include low output power at idle speeds, high transient load-dump overvoltages (up to 80V) and brush life.

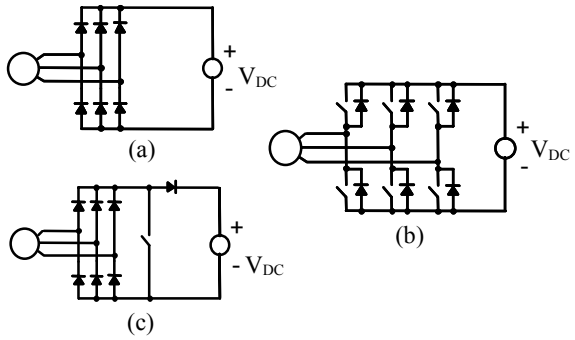

Fig. 1. a) 3-ph rectifier, b) inverter drive, c) switched-mode rectifier.

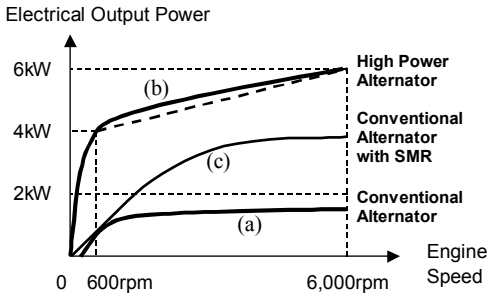

Fig. 2. Alternator output power versus engine speed, a) conventional alternator, b) high power alternator requirements, and c) conventional alternator with switched-mode rectifier (SMR).

A. High Power Alternator Requirements

Proposed new features in cars, such as electromechanical valves and active suspension systems, will increase the auxiliary electric power consumption and hence require a higher power alternator. It is predicted that in the near future the electrical load on the alternator will increase to about 4 to 6kW in luxury cars [2]. This is in parallel with the proposal for a new 42V system voltage in cars.

An example output specification [1] for such a high power alternator is 4kW at idle (600rpm engine speed) rising linearly to 6kW at maximum speed (6,000rpm) as shown in Fig 2b. This represents a challenging 10:1 constant power speed range.

Other requirements include high system efficiency (at least 75% at 3kW output at cruising speed of 1,800rpm), low system cost, a capability of safe overspeed operation to 10,000rpm, and fast transient response to minimize load-dump over-voltages. If a starting function is also incorporated into the alternator, this should be capable of 150Nm of starting torque.

B. Inverter-Driven Alternators

The majority of present research work has focussed on using a brushless inverter-driven machine (see Fig 1b) acting as both a starter and a high power alternator, producing the term "integrated starter/alternator" (ISA). An ISA represents an attractive stepping stone to a hybrid vehicle. Researchers have examined the implementation of an ISA using induction machines, switched-reluctance machines, surface permanent magnet (PM), and interior PM machines [1,3-5].

The conventional alternator and starter have a total cost of approximately US$100. An inverter-driven ISA is considerably more expensive than this. This is largely due to the cost of the inverter which can exceed the cost of the machine by a factor of over 5:1. The estimated costs for an ISA system exceed US$500 [5]. The high cost of the inverter is associated with the number and ratings of the power electronic devices and their associated drivers, the complexity of high speed field-weakening control, and the need for position and current sensors (or sensorless algorithms).

C. Switched-Mode Rectifiers with Conventional Alternators

For alternators based on PM machines it is possible to use a 3-ph switched-mode (or boost) rectifier (see Fig. 1c), instead of an inverter. This has been used with surface PM machines to produce a regulated output voltage which is greater than the back-emf voltage [6]. This topology makes use of the (generally small) leakage reactance of the surface PM machine to avoid the necessity for an external inductor.

Perreault [7,8] has proposed a means for increasing the available output power from a conventional Lundell alternator by using a switched-mode rectifier to allow the alternator to operate at its maximum output power point over a wide range of speeds and yet still deliver a constant output voltage. Note that conventional alternators have high synchronous reactances and that the output voltage from the switched-mode rectifier in this case can be either higher or lower than the back-emf voltage.

Perreault's results show a substantial output power improvement at higher speeds (see Fig. 2c) compared with the conventional rectifier, though it does not meet the high power alternator requirements. Despite this, his proposal is attractive as a low-cost, short-term means for obtaining more output power from conventional alternators. Note that there are still remaining issues, with limitations on the brushes, power output at idle speeds, and the system efficiency.

D. Uncontrolled Generation

The proposed inverterless approach utilises what was previously considered a fault mode of inverter-driven PM machines called uncontrolled generation.

Consider an inverter-driven PM machine (see Fig. 1b) operating as a motor at high speed where the induced back-emf voltages exceed the supply voltage. A controller fault occurs which disables the inverter switches, leaving only the free-wheeling diodes (see Fig. 1a). The high back-emf voltages now cause the machine to act as a generator.

This situation is normally undesirable as the resultant high generating currents could damage the machine or cause system overvoltages if the DC bus is unable to absorb the regenerated power. For this reason, it is considered desirable that the back-emf voltage of PM machines at maximum speed be kept lower than the rated output voltage [9].

Uncontrolled generation was described initially by Adnanes [10]. Later, Jahns et al. [9,11] performed a detailed study of this effect. They showed that for analysis purposes, the DC voltage source in Fig. 1a could be approximated as a resistive load (see Fig. 3a) and the configuration further simplified to a 3-ph resistive load (see Fig. 3b).

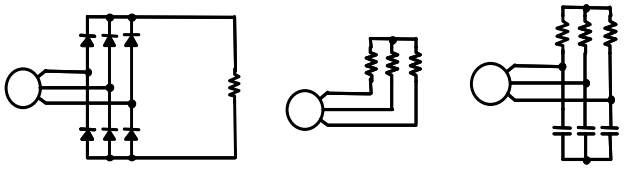

Fig. 3. An alternator with different output loads, a) 3-ph rectifier/resistive load, b) 3-ph resistive load, and c) 3-ph parallel resistive/capacitive load.

E. Inverterless Concept

This paper arose from research into means for testing the field-weakening performance of interior PM machines without an inverter. A key point was the realization that in an inverter-driven PM generator, the inverter is effectively acting as a variable load impedance (normally with leading power-factor). Thus at a particular speed and generating load, the inverter can be replaced by a passive load with the same equivalent resistance and capacitance (see Fig. 3c). Note that removing the capacitors yields the 3-ph resistive load in Fig. 1b which Jahns has shown to be equivalent to uncontrolled generation.

The proposed inverterless concept is based on operating an optimised interior PM machine with the switched-mode rectifier arrangement used by Perreault. This avoids the complexity and high cost of an inverter. It also eliminates the need for a position sensor, minimizes the power electronic switch VA ratings, and has simple control requirements. Note that in the inverterless arrangement, ideally the switch will not see any more than the rated output voltage or current.

The machine costs for the inverterless arrangement should be comparable to inverter-driven machines; however, the cost of the power electronics and control should be much lower than for an inverter. Thus the cost of an inverterless system is expected to be closer to the conventional alternator than to the inverter solution.

II. Inverterless Operation of Interior PM Machines

An analysis of the performance and optimization of inverterless interior PM machines is described in this section.

A. Alternator Characteristics with Resistive Load

Based on the discussion in the previous section, a convenient first step is to examine the performance of interior PM machines with a 3-ph resistive load. The output current and power versus output voltage loci can be obtained by solving the interior PM machine's steady-state equations for a variable resistive load [9,12]. Assuming a lossless, magnetically linear model, it can be shown that when these curves are normalised to the machine's short-circuit current and open-circuit voltage, their shape is not affected by speed and depend only on the machine's saliency ratio (see Fig. 4).

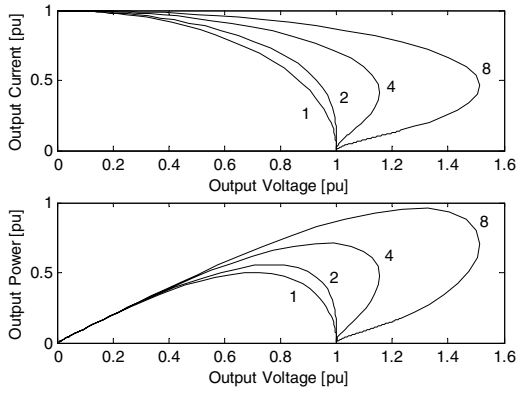

Fig. 4. Ideal normalised current and power versus voltage loci for interior PM machines with a 3-ph resistive load for saliency ratios of 1, 2, 4, and 8.

For a saliency ratio of unity, that is, a surface PM machine, the machine equivalent circuit corresponds to a voltage source with a series reactance. With a resistive load, this yields the semi-circular output current-voltage locus shown in Fig. 4. Maximum power occurs with an output current of

about 70% of the short-circuit current. Note that as the saliency ratio is increased from unity, the maximum output power increases significantly.

For saliency ratios exceeding two, the curve develops an increasing voltage overshoot, that is, the output voltage under load is initially higher than the open-circuit voltage. This characteristic is responsible for the bistable or hysteresis effect during uncontrolled generation which was observed by Jahns [9]. For saliency ratios below 0.5 (not shown), a current overshoot occurs where the output current under load can initially exceed the short-circuit current.

Fig. 5 shows a good correspondence between the calculated and measured characteristics of the concept demonstrator interior PM alternator (described in Section III) with a 3-ph resistive load at two speeds. This machine has an unsaturated saliency ratio of approximately 6. The calculated curve includes the effect of stator resistance and magnetic saturation, which has reduced the predicted voltage overshoot to about 10% compared with over 30% which was expected from interpolating the curves in Fig. 4. This reduction is largely due to the heavy magnetic saturation in this alternator (see Fig. 9).

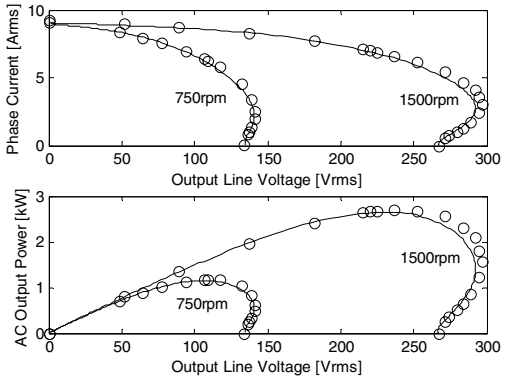

Fig. 5. Plot of current and power versus voltage curves for the concept demonstrator machine at two speeds with a 3-ph resistive load. Calculated results (lines) and experimental results (circles).

It is interesting to consider how the shape of the current-voltage loci shown in Fig. 5 vary with speed. The permanent magnet flux causes the open-circuit voltage to be proportional to speed. As the machine reactances are also proportional to speed, the short-circuit current should thus be independent of speed (ignoring stator resistance). Thus if the back-emf voltage is large compared with the output voltage, then the output current will not be significantly affected by speed and the alternator can be modelled by a constant current source. This is opposite to "traditional" PM generators which are normally treated as voltage sources whose output voltage is proportional to speed.

An alternator with a constant output current can be controlled by a switched-mode rectifier (see Fig. 1c) to produce a regulated DC output voltage. The duty-cycle of the switch determines what fraction of the alternator output current is fed to the load.

In order to fully utilise this constant current characteristic, the machine should be designed with a back-emf voltage which is much larger than the rated output voltage, and a short-circuit current which is equal to the rated output current. Consequently the machine should have both high back-emf voltage and high reactance. This is similar to the characteristics of the conventional Lundell alternators used by Perreault. Note that making the short-circuit current equal to the rated current has been shown to give the best field-weakening performance in PM machines [13,14].

B. Normalisation Procedure

The effect of the choice of the interior PM machine parameters on the output power versus speed characteristics under both inverter and inverterless operation will now be examined. A lossless, linear model will again be used and only machine designs where the short-circuit current is equal to rated current will be considered (henceforth referred to as optimal designs). In other words, it is assumed that the magnet stator flux-linkage Ψ_m and the d-axis inductance L_d will be chosen so that $\Psi_m=L_dI_0$ where I_0 is the rated current.

The two design parameters for optimal interior PM machines which will be used in this analysis are the saliency ratio $\xi=L_q/L_d$ (where L_q is the q-axis inductance), and the back-emf ratio $\kappa=E/V_0$. The back-emf ratio is the ratio of the back-emf voltage $E=\Psi_m\omega$ at the rated speed ω_0, to the rated voltage V_0. In previous work [13], the rated speed was chosen to be the highest speed at which rated torque could be produced; however, in this paper the rated speed will be chosen to be the maximum speed in the CPSR.

Applying the above normalisation yields the normalised magnet flux-linkage $\Psi_{mn}=\kappa$, normalised d-axis inductance $L_{dn}=\kappa$ and normalised q-axis inductance $L_{qn}=\xi\kappa$. It will be assumed that the rated machine output voltage and current cannot be exceeded. Using these results, the output power characteristics of optimal interior PM machines can now be calculated using the approach given in [13] for inverter operation and in [9,10,12] for inverterless operation.

C. Optimal Surface PM Machines

Fig. 6 shows the normalised output power versus speed characteristics of surface PM machines (i.e. $\xi=1$) for various back-emf ratios κ for both inverterless and inverter operation.

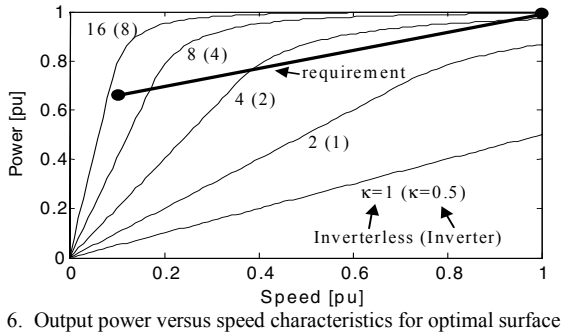

Fig. 6. Output power versus speed characteristics for optimal surface PM alternators as a function of the back-emf ratio κ, under inverterless operation. The corresponding back-emf ratio for inverter operation is shown in brackets. The high power alternator requirement is also indicated.

The electrical power versus speed curves initially linearly increase (representing constant input torque) up to an output power of about 0.7pu, and then asymptote towards 1pu for higher speeds. The shape of all the curves are identical and hence each curve can be defined by only its initial slope. This initial slope is the maximum input torque capability of the alternator at rated current, and is linearly proportional to the back-emf ratio κ (that is, the magnet flux).

For a surface PM alternator of a given back-emf ratio, it can be shown that the maximum input torque under inverter operation is twice that achievable under inverterless operation. This is because of the greater control flexibility available with inverter operation. Thus the output curve for inverterless operation at a back-emf ratio of, say, 16 corresponds to the curve for inverter operation with a back-emf ratio of 8. Alternatively, to achieve the same output power characteristic, inverterless operation requires an alternator with twice the back-emf ratio as that required for inverter operation.

The high power alternator requirement is 4kW at 600rpm linearly increasing to 6kW at 6,000rpm. Normalising this gives a requirement of 2/3pu output power at 0.1pu speed increasing to 1pu output power at 1pu speed. To achieve this, from Fig. 6 it can be shown that an inverter-driven surface PM machine requires a high back-emf ratio of 6.67 while the inverterless configuration requires an even higher back-emf ratio of 13.33.

D. Optimal Interior PM Machines

With the high power alternator requirement in mind, it is convenient to define the constant power speed range (CPSR) of an interior PM alternator as the speed range over which the output power is greater than 2/3pu. Thus the high power alternator requirement is a CPSR of 10. As 2/3pu output power corresponds to operation in the constant input torque region (i.e. less than about 0.7pu output power), then the CPSR can be found from the maximum input torque. For inverter operation, the maximum input torque corresponds to operation at the maximum torque per ampere point [13]. For inverterless operation, the maximum input torque can be found by differentiating the relation given in [12] relating the input torque to the value of load resistance.

Fig. 7 shows contour plots of the CPSR for optimal interior PM machines as a function of the back-emf ratio and the saliency ratio for both inverter and inverterless operation. The x-axis corresponds to a saliency ratio of unity (surface PM alternators) which was considered in Fig. 6. Note that for surface PM machines, the CPSR for inverter operation is twice that for inverterless operation.

For a given back-emf ratio, increasing the saliency ratio significantly improves the CPSR; however, the improvement is much greater for inverter than for inverterless operation.

Note that to achieve a CPSR of 10 with an inverter-driven machine, the normal design requirement to keep the back-emf at maximum speed at less than the rated voltage [9] (i.e. back-emf ratio $\kappa < 1$) would require a very high saliency ratio of about 13.

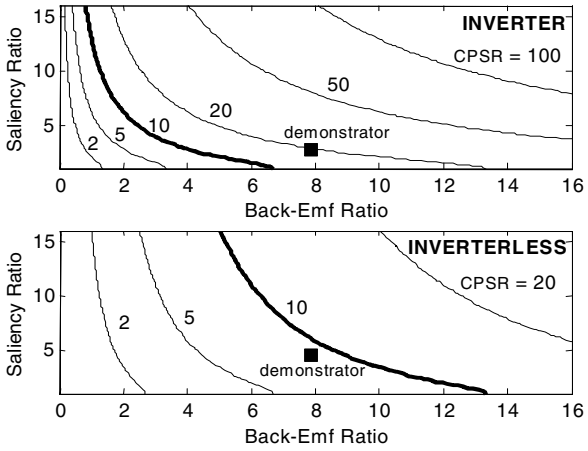

Fig. 7. CPSR contour plots for optimal interior PM machines as a function of back-emf ratio and saliency ratio, for inverter and inverterless operation. The high power alternator requirement of a CPSR of 10 is highlighted. The location of the concept demonstrator design is shown as a square.

The location of the concept demonstrator design is shown as a square in Fig. 7 using the measured back-emf ratio of 7.8 and calculated saturated saliency ratio of 2.7 for inverter operation and 4.6 for inverterless operation (from the measured flux-linkages curves in Fig. 9). Experimental results for this machine are presented in the next section.

III. Concept Demonstrator Machine

Earlier, the authors constructed a multiple-barrier interior PM rotor (see Fig. 8) for a commercial 4 pole, 2.2kW, 415V, 50Hz induction machine stator. The rotor was initially tested with ferrite magnets and the results reported in [12,15]. These have now been replaced with rare-earth (NdFeB) magnets to increase the magnet flux. Though this machine was not specifically designed for this purpose, it provides a useful concept demonstrator for a belt-driven (3:1 ratio) high power automotive alternator. Note that though the voltage rating of this machine is much larger than the alternator requirement, rewinding it for a lower voltage (and hence higher current) will not change its output power or efficiency characteristics.

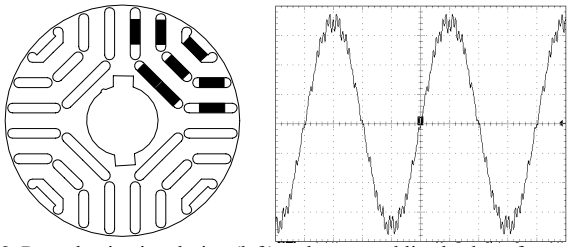

Fig. 8. Rotor lamination design (left) and measured line back-emf waveform at 1,500rpm with NdFeB magnets (right). The line voltage is 271Vrms.

A. Parameter Measurement

The measured inductance saturation parameters of the machine are shown in Fig. 9 for the machine without magnets (reluctance), with ferrite magnets and then with NdFeB

magnets. The induction machine stator was rated at 4.8A and the inductances have been measured at currents up to twice this value. This causes heavy saturation in the q-axis of the machine. The addition of magnet flux in the d-axis produces a cross-saturation effect which reduces the q-axis inductance. This is relatively small with ferrite magnets but significant with NdFeB magnets.

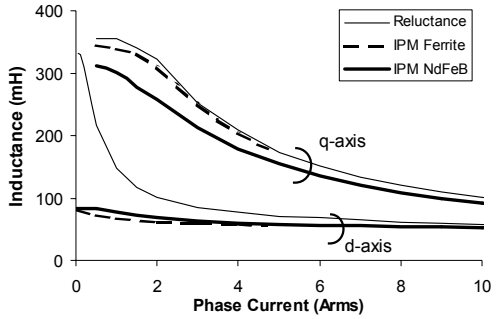

Fig. 9. Measured d-axis and q-axis inductance saturation curves for the machine without magnets, with ferrite magnets and with NdFeB magnets.

The d-axis curves are strongly affected by saturation of rotor bridges (see Fig. 8) when no magnets are present. In the PM machines, the magnet flux saturates the rotor bridges and so produces a relatively constant d-axis inductance.

Fig. 8 also shows the measured back-emf waveform of the machine with NdFeB magnets. Assuming a maximum speed of 18krpm with a 3:1 belt ratio, this gives a very high back-emf ratio of nearly 8 (see Table 1).

TABLE 1
COMPARISON OF ROTORS IN 415V, 2.2KW INDUCTION MOTOR STATOR

	Reluctance	**IPM Ferrite**	**IPM NdFeB**
Magnet Type	-	ferrite	NdFeB
Line Back-EMF at 1,500rpm	0	83V	271V
Short-Circuit Current	0	2.2A	9.3A
Back-EMF at 18krpm	0	1.0kV	3.25kV
Back-EMF ratio κ at 18krpm	0	2.4	7.8
Max Saliency Ratio ξ	3.3	6.1	5.7
Inverterless Output Power	0	≈1.6kW	≈6.9kW

Table 1 also shows the measured high-speed short-circuit current of the PM machines, the maximum saliency ratio (calculated as the unsaturated value of L_q divided by the saturated value of L_d), and the ideal maximum inverterless output power calculated from the rated voltage (415V) and the short-circuit current.

B. Mechanical Strength

A key limitation of the concept demonstrator machine is the mechanical strength of the rotor. The high power alternator specification, assuming a 3:1 belt ratio, requires a rated alternator maximum speed of 18krpm and an overspeed capability of 30krpm [1].

The failure speed of the concept demonstrator has been roughly estimated to be in the order of 12 to 15krpm. This could be improved by optimising the location, number and thickness of the rotor ribs [16] and by carefully selecting the heat-treatment of the laminations to trade-off magnetic properties for improved mechanical strength [17].

C. Dynamometer Arrangement

The interior PM concept demonstrator was driven by two 5kW, 1,500rpm DC machines through a belt drive with adjustable gear ratios of 1:1, 1:2 and 1:4 which gave a maximum speed of 6,000rpm. A 220V/50A variable DC power supply was used to drive the DC machines. The reaction torque on the alternator stator was measured using a load cell.

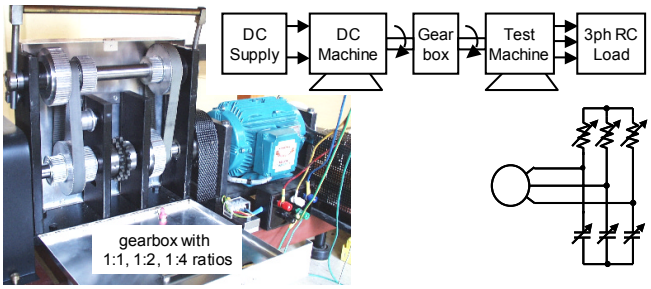

Fig. 10. Block diagram of experimental set-up, photograph of the gearbox and concept demonstrator machine, and the circuit for the 3-ph variable resistive/capacitive load.

The three different load configurations shown in Fig. 3 were produced using combinations of a 3-ph rectifier, three 240V/20A single-phase variable resistance banks and a 3-ph 440V/120uF variable capacitance bank. The capacitance bank could be connected in star (to give a range of 0 to 120uF, 0.5uF steps) or delta (to give a range of 0-360uF, 1.5uF steps). Higher capacitance values were achieved by adding external fixed capacitor banks.

Fig. 11 shows an example of the calculated resistance/capacitance values as a function of speed which are required to simulate an inverter. It corresponds to the values used to obtain the results shown in Fig. 14.

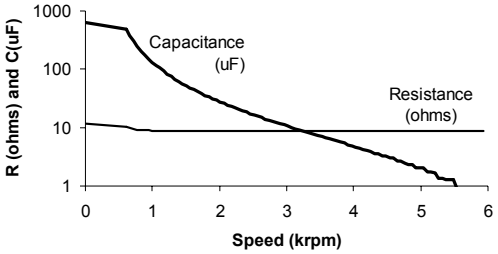

Fig. 11. Calculated 3-ph parallel resistance and capacitance per phase used to produce the "inverter" maximum output power characteristics in Fig. 14.

IV. EXPERIMENTAL TEST RESULTS AND DISCUSSION

In this section the performance of the interior PM concept demonstrator under both inverter and inverterless operation is examined.

A. Inverter-Driven Starting Torque Performance

The engine starting torque requirement is 150Nm. With a 3:1 belt drive this would be equivalent to 50Nm at the starter/alternator.

Fig. 12 shows the torque versus current characteristic with a 3-ph resistive/capacitive load simulating an inverter. The generating torque measurements show a close correspondence to the calculations. The measurements are slightly higher due to iron and windage/friction losses which were not modelled in the calculations. Note that apart from these losses, the motoring and generating torque versus current characteristics should be identical. The results indicate that the required 50Nm starting torque should be achievable with an inverter current of about 12A.

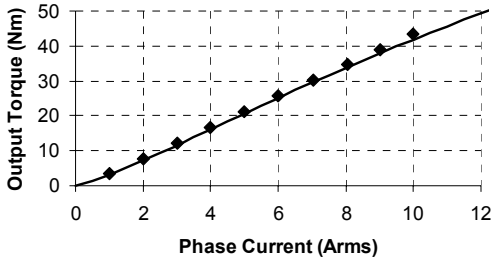

Fig. 12. Concept demonstrator torque versus current characteristic. Calculated characteristic based on the measured machine parameters (solid line) and measured generating torque with 3-ph RC load (diamonds).

B. Generating Output with Three-Phase R and RC Loads

The concept demonstrator alternator was tested using a 3-ph resistive load to simulate inverterless operation and a 3-ph resistive/capacitive load to simulate inverter operation at alternator speeds of up to 6,000rpm (corresponding to an engine speed of 2,000rpm). The rated current under inverter operation was chosen to be equal to the alternator short-circuit current (9.3A).

Tests were performed at rated line voltage (415V) to verify the low speed output power capability (see Fig. 13). However, the 6,000rpm dynamometer speed restriction meant that the expected 10:1 CPSR could not be demonstrated. Thus, further tests at one-third rated line voltage were necessary to verify the CPSR (see Fig. 14).

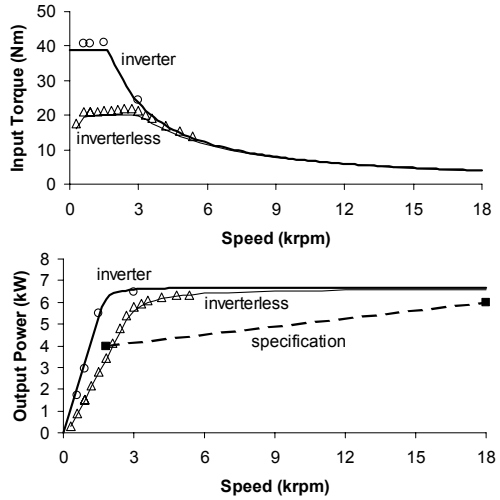

Fig. 13. Torque and power versus speed curves at rated voltage showing the measurements under "inverter" (circles) and "inverterless" (triangles) operation, the calculated curves (lines) and the alternator specification.

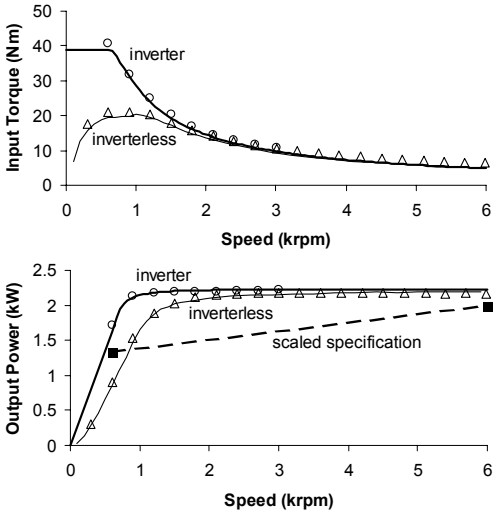

Fig. 14. Torque and power versus speed curves at one-third rated voltage showing the measurements under "inverter" (circles) and "inverterless" (triangles) operation, the calculated curves (lines) and the "scaled" alternator specification.

The calculated results shown in Figs. 13 and 14 used the measured interior PM machine parameters and included the effect of stator resistance and magnetic saturation but not iron or friction/windage losses.

The measured output power under both inverter and inverterless operation shows an excellent correspondence with the calculations. The measured input torque is slightly higher than predicted due to iron and friction/windage losses which were not modelled.

Fig. 13 shows that the concept demonstrator easily meets the idle power requirement associated with the 10:1 CPSR specification under inverter operation, and nearly meets it under inverterless operation. These results correspond well with the location of its design parameters on the CPSR contour plots shown in Fig. 7. Note that at low speeds, the output power under inverter operation is about twice that under inverterless operation but that they asymptote to the same value at high speeds.

In Fig. 14 the machine was tested at one-third rated voltage in order to demonstrate its CPSR. A one-third scaled specification is shown for reference. Even with the loss of performance at the lower voltage due to the more pronounced effect of stator resistance, the machine demonstrates an outstanding CPSR which exceeds the 10:1 specification under inverter operation and is close to meeting it under inverterless operation. The drop in the inverterless input torque (and hence output power) at very low speeds is due to stator resistance.

C. Losses and Efficiency

Fig. 15 shows the measured losses as a function of speed for the inverterless (resistive load) operation corresponding to the output power versus speed curves in Figs. 13 and 14. It shows both the total losses and the losses after stator copper losses are removed leaving the friction/windage and iron losses.

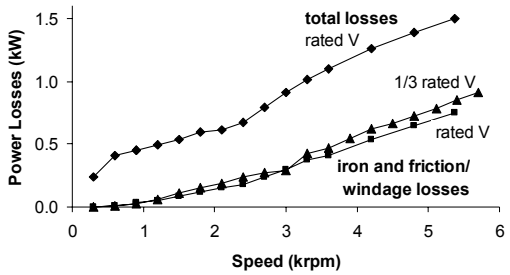

Fig. 15. Measured losses under "inverterless" operation for the concept demonstrator. The total losses are shown at rated voltage. The iron and friction/windage losses are shown at both rated and one-third rated voltage.

The iron and friction/windage losses show an approximately square law relationship with speed. At 6krpm they are roughly equal to the stator copper losses. This result is a major concern for a machine which is required to operate up to 18krpm. As the outside of the rotor is smooth, the windage losses should be relatively low. It is therefore assumed that the majority of these losses are iron losses.

The high iron losses are likely to be due to the high flux densities in the machine. Though the stator currents reduce the fundamental component of the airgap magnetic field in the machine at high speeds, significant harmonic components may still be present which could cause large losses. This is consistent with Fig. 15 which shows the losses are not significantly affected by the output voltage.

The losses could be reduced by means such as : lowering the required back-emf voltage by optimizing the machine to improve its saliency ratio (see Fig. 7); redesigning the machine to reduce the harmonic flux components; and using thinner and lower loss lamination material [17].

Note that the measured electrical output power in the one-third rated voltage test (Fig. 14) is close to the calculated values despite nearly 1kW of unmodelled iron and friction/windage losses. It thus appears that these losses increase the required mechanical input power but do not significantly affect the electrical output power.

Fig. 16 shows the measured efficiency of the alternator at the full-load, rated voltage conditions shown in Fig. 13 for both inverter and inverterless operation. The efficiency at a given speed under the two modes of operation is surprisingly similar despite the considerable difference in output power between them, particularly at lower speeds. At higher speeds the efficiency was expected to remain constant. The measured fall in efficiency is due to the high extra losses shown in Fig. 15.

D. Generating with Diode Rectifier/Voltage Source

The alternator was also tested while operating through a diode rectifier into a DC voltage source (see Fig. 1a). The waveforms in Fig. 17 show operation at both low and high speeds. It is interesting to observe that they resemble the waveforms in brushless PM motors when driven from a six-step inverter. The waveforms correspond well to those observed earlier by Adnanes [10].

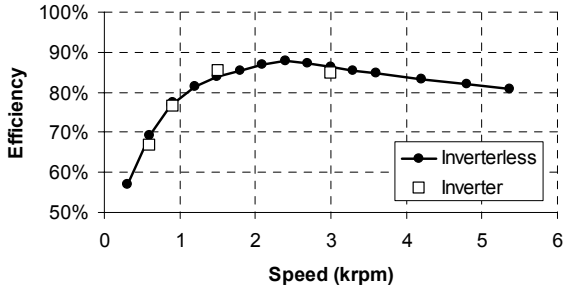

Fig. 16. Measured efficiency at rated voltage of the concept demonstrator corresponding to the power output curves shown in Fig. 13.

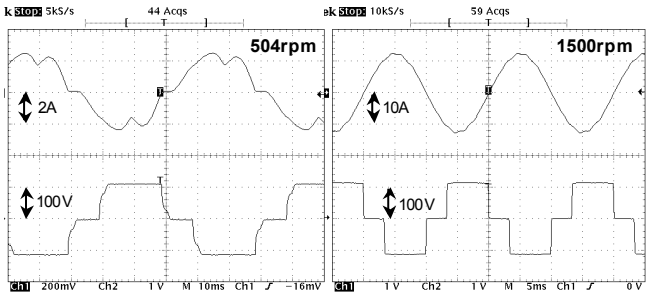

Fig. 17. Measured generating waveforms with the alternator operating through a diode rectifier into a 110V DC voltage source at low and high speeds. Alternator phase current (upper) and line voltage (lower).

E. Generating with Diode Rectifier/Resistive Load

The output power tests in Figs. 13 and 14 have used 3-ph passive loads and so a final test was used to verify the alternator output power characteristics when operating through a diode rectifier into a resistive load (see Fig. 3a). Fig. 18 shows both the machine AC output and the rectifier DC output characteristics. Note that the equivalent AC output voltage for a given DC output voltage was calculated from the fundamental component of the ideal six-step voltage waveform shown in Fig. 17.

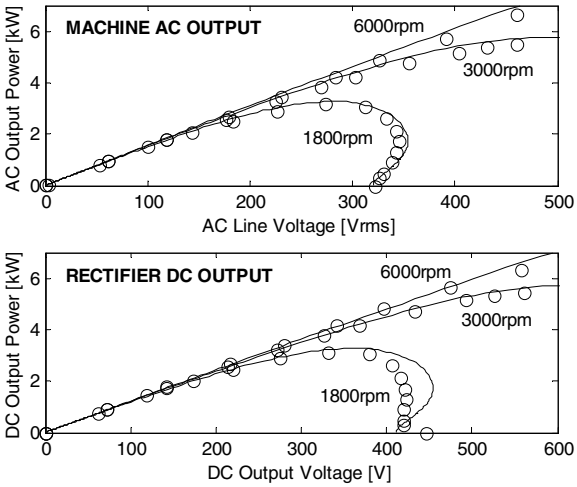

Fig. 18. Concept demonstrator performance when driving a resistive load through a rectifier. Top graph shows the machine AC output power versus AC line voltage and lower graph shows the rectifier DC output power versus DC output voltage. Measured (circles) and calculated (solid lines).

The results confirm that the machine is capable of delivering the required 6kW DC output power. The AC

characteristics closely follow the calculated curves while the DC characteristics show some significant deviations at low currents where the current waveform is discontinuous. The DC output voltage rises unexpectedly on open-circuit, possibly due to the harmonics in the open-circuit voltage (see Fig. 8).

V. Conclusions

This paper has investigated a low-cost means of implementing a 6kW brushless automotive alternator with a 10:1 constant power speed range (CPSR) without an inverter. The key results of this paper are :

- a high back-emf, high reactance permanent magnet (PM) alternator can efficiently produce a regulated DC output voltage over a wide CPSR using a switched-mode rectifier (referred to as inverterless operation)
- the optimum design for wide CPSR operation for inverterless (and inverter-driven) PM alternators is to choose the magnet flux and d-axis inductance such that the short-circuit current is equal to the rated output current
- for optimal interior PM alternator designs, the CPSR is determined by the back-emf ratio (the ratio of the back-emf voltage at maximum speed to the rated output voltage), and the saliency ratio
- inverterless operation gives lower output power at low speeds than inverter operation (and hence poorer CPSR) but the same high speed output power
- for a given CPSR with an optimal interior PM machine, increasing the saliency ratio reduces the required value of back-emf ratio; however, the effect is much larger for inverter operation than for inverterless operation
- an extensive series of tests on an interior PM concept demonstrator machine has validated the theoretical results and it was demonstrated that this machine can deliver 6kW at high efficiency over an extremely wide CPSR
- areas for further work include : reducing the high observed iron losses, improving the rotor mechanical speed capability, implementing the power electronics and control, and demonstrating operation on a car engine

In summary, it has been shown that a high back-emf, interior PM alternator with a switched-mode rectifier offers a promising low-cost, high-efficiency alternative to an inverter drive for applications such as high power automotive alternators which require a wide CPSR.

VI. Acknowledgment

This work was supported by a 2001 University of Adelaide Small Research Grant and a 2003 Australian Research Council Discovery Projects Grant. Thanks to the staff of the School's mechanical workshop for construction of the dynamometer and to C.Z. Liaw for support in the testing. Technical discussions with E.C. Lovelace, T.M. Jahns and B.A. Welchko are also gratefully acknowledged.

VII. References

[1] E.C. Lovelace, "Optimization of a Magnetically Saturable Interior Permanent-Magnet Synchronous Machine Drive," Ph.D. Thesis, Massachusetts Institute of Technology, June 2000.

[2] J.G. Kassakian, J.M. Miller and N. Traub, "Automotive Electronics Power Up," IEEE Spectrum, May 2000, pp. 34-39.

[3] J.M. Miller, A.R. Gale, P.J. McCleer, F. Leonardi and J.H. Lang, "Starter-Alternator for Hybrid Electric Vehicle: Comparison of Induction and Variable Reluctance Machines and Drives," IEEE Industry Applications Society Annual Meeting, 1998, pp. 513-523.

[4] F. Caricchi, F. Crescimbini, E. Santini and L. Solero, "High-Efficiency Low-Volume, Starter/Alternator for Automotive Applications," IEEE Industry Applications Society Annual Meeting, 2000.

[5] E.C. Lovelace, T.M. Jahns, J.L. Kirtley and J.H. Lang, "An Interior PM Starter Alternator for Automotive Applications," Int. Electric Machines and Drives Conference, Turkey, vol. 3, 1998, pp. 1802-1808.

[6] G. Venkataramanan, B. Milkovska, V. Gerez and H. Nehrir, "Variable Speed Operation of Permanent Magnet Alternator Wind Turbines Using a Single Switch Converter," Journal of Solar Energy Engineering, vol. 118, Nov. 1996, pp. 235-238.

[7] D.J. Perreault and V. Caliskan, "Automotive Power Generation and Control," Massachusetts Institute of Technology, LEES Technical Report, May 2000.

[8] D.J. Perreault and V. Caliskan, "A New Design for Automotive Alternators," IEEE SAE International Conference on Transportation Electronics (Convergence), Detroit, MI, Oct. 2000.

[9] T.M. Jahns and V. Caliskan, "Uncontrolled Generator Operation of Interior PM Synchronous Machines Following High-Speed Inverter Shutdown," IEEE Trans. Industry Applications, vol. 35, no. 6, Nov./Dec. 1999, pp. 1347-1357.

[10] A.K. Adnanes, R. Nilssen and R.O. Rad, "Power Feed-Back During Controller Failure in Inverter Fed Permanent Magnet Synchronous Motor Drives with Flux-Weakening," IEEE Power Electronics Specialists Conference, 1992, pp. 958-963.

[11] V. Caliskan, D.J. Perreault, T.M. Jahns and J.G Kassakian, "Analysis of Three-Phase Rectifiers with Constant-Voltage Loads," IEEE Power Electronics Specialists Conference, 1999, pp. 715-720.

[12] B.A. Welchko, T.M. Jahns, W.L. Soong and J.M. Nagashima, "IPM Synchronous Machine Drive Response to Symmetrical and Asymmetrical Short Circuit Faults," IEEE Trans. Energy Conversion, vol. 18, no. 2, Jun. 2003, pp. 291-298.

[13] W.L. Soong, "Design and Modelling of Axially-Laminated Interior Permanent Magnet Motor Drives for Field-Weakening Applications," Ph.D. Thesis, University of Glasgow, 1993.

[14] W.L. Soong and T.J.E. Miller, "Field-Weakening Performance of the Five Classes of Brushless Synchronous AC Motor Drives," IEE Proceedings, Electric Power Applications, vol. 141, no. 6, Nov. 1994, pp. 331-340.

[15] W.L. Soong, N. Ertugrul, E.C. Lovelace, T.M. Jahns, "Investigation of Interior Permanent Magnet Offset-Coupled Automotive Integrated Starter/Alternator," IEEE Industry Applications Society Annual Meeting, 2001, pp. 429-436.

[16] E.C. Lovelace, T.M. Jahns, T.A. Keim and J.H. Lang, "Mechanical Design Considerations for Conventionally-Laminated, High-Speed Interior PM Synchronous Machine Rotors," IEEE IEMDC, Cambridge, 2001, pp. 163-169.

[17] W.L. Soong, G.B. Kliman, R.N. Johnson, R. White and J. Miller, "Novel High Speed Induction Motor for a Commercial Centrifugal Compressor," IEEE Trans. Industry Applications, vol. 36, no. 3, May/Jun. 2000, pp. 706-713.